NANO LETTERS

2004
Vol. 4, No. 5
859−862

Quantitative Analysis of Scanning Conductance Microscopy

Cristian Staii and Alan T. Johnson, Jr.*

Department of Physics and Astronomy and Laboratory for Research on the Structure of Matter, University of Pennsylvania, Philadelphia, Pennsylvania 19104

Nicholas J. Pinto

Department of Physics and Electronics, University of Puerto Rico, Humacao, Puerto Rico 00791

Received February 13, 2004

ABSTRACT

We present a quantitative model for phase shifts observed in scanning conductance microscopy and show excellent agreement with data on samples of (conducting) single wall carbon nanotubes and insulating poly(ethylene oxide) (PEO) nanofibers. The model takes into account phase shifts due to the electrostatic (capacitive) forces exerted on the tip by sample and substrate, using simple approximate geometries. Data for large diameter, conducting doped polyaniline/PEO nanofibers are qualitatively explained. This quantitative approach is used to determine the dielectric constant of PEO nanofiber, a general method that can be extended to other dielectric nanowires.

Scanning conductance microscopy (SCM) is a useful scanning probe technique that can be used to investigate the conductance of nanoscale samples with no need for electrical contacts. SCM was previously used to image single-wall carbon nanotubes (SWNTs), to demonstrate the insulating character of λ-DNA at the micrometer scale,[1] and to distinguish between conducting and insulating polyaniline/poly(ethylene oxide) (PAn/PEO) nanofibers.[2] An SCM image records the oscillation phase of a driven voltage-biased AFM cantilever as a function of the tip position (Figure 1a). Earlier results[2] show that, in SCM, carbon nanotubes always show a negative phase shift (Figure 1b), while insulating poly-(ethylene oxide) (PEO) nanofibers show a positive phase shift that increases with fiber diameter (Figure 1c). We have also reported[2] that conducting doped polyaniline/poly(ethylene oxide) (PAn/PEO) fibers with diameter larger than 30 nm show a negative-positive-negative ("double dark line") contrast in SCM (Figure 1d). Although a model for SCM has previously been proposed,[1] it does not account for all these observations.

Here we present an improved model for SCM that explains these observations quantitatively *and* significantly enhances the analytic power of the technique. We show explicitly how calculations of the phase shift that forms the SCM image, determined by the total capacitance of the tip−sample-substrate system, are in excellent agreement with data from samples of SWNTs and PEO nanofibers. Moreover, we then use SCM to measure the dielectric constant of the insulating PEO nanofibers. Finally, we provide a semiquantitative explanation for the negative-positive-negative phase shift observed for conducting PAn/PEO nanofibers.

For the SCM measurements we use CVD grown SWNTs,[3] insulating poly(ethylene oxide) (PEO) nanofibers, and conducting nanofibers made from a blend of polyaniline doped with camphorsulfonic acid and insulating poly(ethylene oxide) (PAn.HCSA/PEO).[2] The substrate for all experiments is a 200 nm SiO_2 layer on top of a p-type degenerately doped Si wafer.

SCM is a dual-pass technique. In the first line scan, the tip acquires a topography profile in tapping mode. In the second (interleave) line scan (Figure 1a), the tip travels at a defined height above the surface. A DC voltage is applied to the tip, and the cantilever is mechanically driven at its free oscillation resonant frequency. The SCM image records the phase of the cantilever oscillation as a function of tip position. SCM images were taken on a Digital Instruments Dimension 300 NS-IIIA AFM using W_2C-coated tips (NSC12/W2C, Mikromasch) with curvature radius $R = 30-60$ nm, quality factor $Q = 150$, and spring constant $k = 0.65-1$ N/m. Figure 1 shows SCM images for SWNTs (Figure 1b), an insulating PEO fiber (Figure 1c), and a conducting PAn.HCSA/PEO fiber (Figure 1d) together with the corresponding line scans (inset in Figure 1b−d). SWNTs show a negative phase shift (Figure 1b), whereas the phase shift for insulating PEO fibers is always positive (Figure 1c). SCM measurements on insulating Si nanowires also show a

* Corresponding author. E-mail: cjohnson@dept.physics.upenn.edu.

10.1021/nl049748w CCC: $27.50
Published on Web 04/08/2004

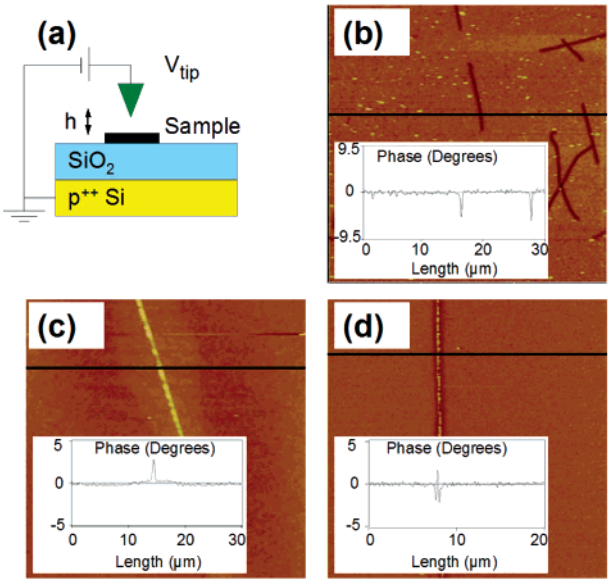

Figure 1. (a) Schematic of SCM. In the interleave scan, the DC voltage-biased AFM cantilever is driven at its resonant frequency at a fixed height h above the sample. The phase of the cantilever oscillation is recorded as a function of tip position. (b) 30 μm × 30 μm SCM image of carbon nanotubes. The inset shows a line scan along the black line. SWNTs and other small diameter conducting nanowires show a *negative* phase shift in SCM. (c) 30 μm × 30 μm SCM image of an insulating PEO nanofiber (diameter 10−100 nm) with a line scan along the black line. Insulating nanofibers show a *positive* phase shift in SCM. (d) 20 μm × 20 μm SCM image of a conducting PAn.HCSA/PEO nanofiber (diameter 100 nm). The inset is a line scan along the black line showing a *negative-positive-negative* contrast in SCM.

positive phase shift (data not shown). Finally, conducting nanofibers with diameter larger than 30 nm show a negative-positive-negative phase shift (Figure 1d).

We explain these images quantitatively by considering a cantilever of resonant frequency ω_0 and spring constant k. For a cantilever driven in air (damping coefficient γ) at frequency ω, the phase shift φ between the driving force and the cantilever oscillation is given by[4,5]

$$\tan(\varphi) = -\frac{\gamma\omega}{\omega_0^2 - \omega^2} \qquad (1)$$

On resonance ($\omega = \omega_0$) the phase shift is $-\pi/2$. We adopt the standard convention of AFM that all measured phase shifts Φ are with respect to this value, that is: $\Phi = \varphi + \pi/2$. SCM images are taken in the interleave mode with tip voltage V_{tip}, and cantilever drive frequency $\omega = \omega_0$. Far from the substrate the phase lag is 0 (Figure 2a). If the cantilever is scanned at height h above a bare SiO_2 substrate, the electrostatic force $F_1(h)$ between metallic tip and surface changes the cantilever resonant frequency by $\Delta\omega$. For small $F_1(h)$, the frequency shift is proportional to the force gradient:[4,5] $\Delta\omega \approx -(\omega_0/2k)F'_1(h)$. If $C_1(h)$ is the capacitance of the tip−substrate system, then $F_1(h) = (1/2)C_1'(h)V_{tip}^2$. The attractive force $F_1(h)$ leads to a decrease of the resonant frequency of

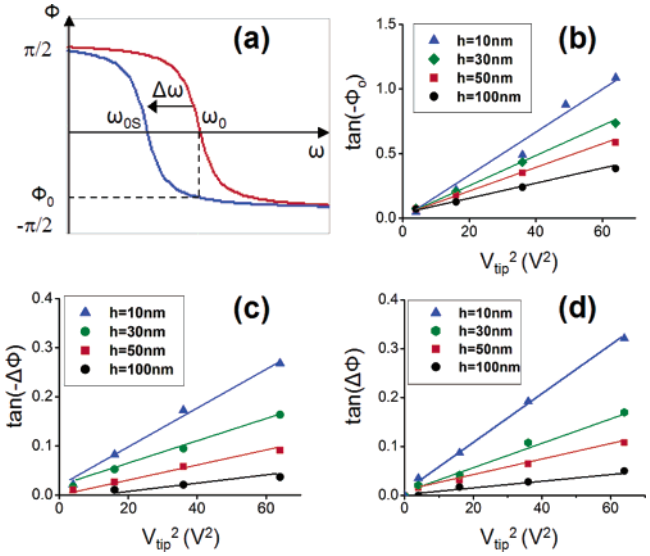

Figure 2. (a) Schematic of phase shift Φ versus cantilever drive frequency ω. Above the substrate, the resonant frequency ω_{0S} is less than the free oscillation resonance, ω_0. The phase-frequency diagram shifts from the red to the blue curve. The cantilever is driven at ω_0 in SCM, so the phase shift takes on a *negative* value Φ_0. (b) Measured $\tan(-\Phi_0)$ as a function of V_{tip}^2, for different scan heights (h = 10−100 nm). A linear relation is seen, as predicted by eq 2. (c), (d) Absolute value of $\tan(\Delta\Phi)$ versus V_{tip}^2 for SWNTs (c) and PEO fibers (d) for different scan heights h. The graphs show a linear relation as predicted by eq 3.

the cantilever (Figure 2a) and therefore to a negative value Φ_0 for the *background* phase lag:

$$\tan(\Phi_0) = -\frac{Q}{2k}C_1''(h)V_{tip}^2 \qquad (2)$$

where $Q = \gamma\omega_0$ is the quality factor of the cantilever. This background value of the phase over the bare substrate is independent of the tip horizontal position and is used as the reference zero in Figure 1b−d.

When the tip is above the sample (SWNT, nanofiber) the total capacitance of the system is $C_2(h)$ with electrostatic force $F_2(h)$. We note that the tip *stays at the same height h* above the sample since it retraces the topography. Again, assuming that the electrostatic forces are small, the phase shift relative to that over the bare substrate is

$$\tan(\Phi - \Phi_0) \approx \frac{Q}{2k}(C_1''(h) - C_2''(h))V_{tip}^2 \qquad (3)$$

Equations 2 and 3 predict that the tangents of both the phase background value and the phase shift above the nanowire vary linearly with V_{tip}^2. This is seen in data taken at different scan heights above the bare SiO_2 substrate, SWNTs, and PEO fibers (Figure 2b−d, respectively). Equation 3 also predicts that the sign of the phase shift in SCM is determined by the change in the second derivative of the total capacitance of the system. To explain the data quantitatively we calculate the capacitances called for in eqs 2 and 3 using a simplified model for the geometry of the bare substrate, a thin SWNT, and a large diameter polymer nanofiber.

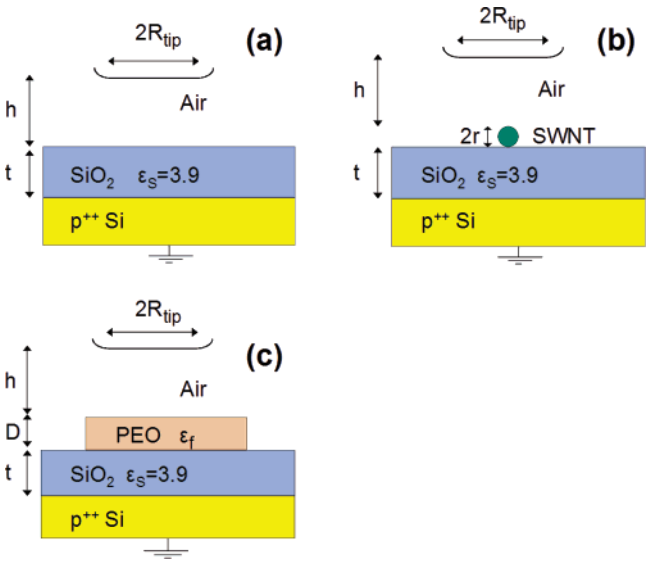

Figure 3. (a)−(c) Models for the tip-sample geometry. The AFM tip (radius $R_{tip} = 30-50$ nm) scans at a constant height h above the sample. (b) The SWNT is approximated with a cylinder of radius $r = 1$ nm and length $L = 1-10$ μm at distances h, t from the tip and Si substrate respectively, both modeled as conducting plates. (c) The PEO fiber is modeled as a dielectric plate of thickness $D = 10-100$ nm. These models are in excellent agreement with the experimental data for intermediate scan heights: $h = 30-50$ nm.

In each case we approximate the SCM tip with a circular parallel plate of radius $R_{tip} = 30-50$ nm. For SCM over the bare substrate, the tip sits a distance h above the SiO_2 dielectric layer (thickness $t = 150-200$ nm) on top of a ground plane (Figure 3a). SWNTs are treated as cylindrical wires of radius $r = 1$ nm and length L (determined for each SWNT by AFM) at distances h and t from two conducting planes (Figure 3b). Since the PEO fiber diameter D is comparable to the tip radius R_{tip}, we model the PEO fiber as an insulating plate of thickness D and dielectric constant ϵ_f (Figure 3c). Even these simple models of the sample geometry give very good agreement with the data (see below), and the accuracy could likely be improved through the use of more realistic geometries.

These models are appropriate for intermediate scan heights of 30−50 nm. For heights $h < 20$ nm, other effects (stray capacitance, static charges on the surface) make significant corrections to the capacitive force considered in the model.[6,7] For tip−sample separation greater than 50 nm, the approximation of the tip as a metallic plate is no longer appropriate and the observed phase shifts are better described by modeling the tip−substrate system as a sphere above a dielectric plane. In the following we therefore restrict our observations to intermediate scan heights (30 nm $< h <$ 50 nm), and we show that within this range the predictions of the geometric models are in excellent quantitative agreement with the data.

Over the bare substrate, the model presented in Figure 3a predicts

$$C_1''(h) = 2\epsilon_0(\pi R_{tip}^2)\frac{1}{(h + t/\epsilon_S)^3} \qquad (4)$$

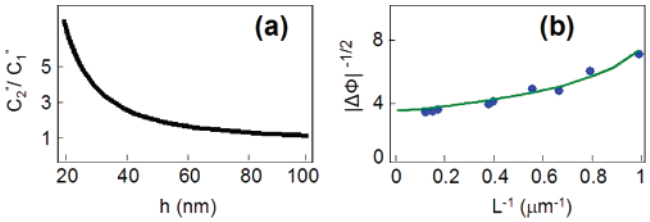

Figure 4. (a) Calculated $C_2''(h)/C_1''(h)$, as a function of scan height h. $C_2''(h) > C_1''(h)$ for the whole range $h = 10-100$ nm, so eq 3 predicts a negative phase shift for SWNTs. (b) $|\Delta\Phi|^{-1/2}$ versus L^{-1}. The green curve represents the theoretical prediction based on the model of Figure 3b and eq 3, and the blue dots are data for $h = 30$ nm and $V_{tip} = +5$ V.

where $\epsilon_S = 3.9$ is the SiO_2 dielectric constant. For $h = 30$ nm, $t = 190$ nm, we find $C_1'' = 102$ $\mu F/m^2$; the experimental value (from the slope of the line in Figure 2b, and using eq 2) is $C_1'' = 95$ $\mu F/m^2$. We repeat this analysis for $h = 50$ nm, and find that: $C_1'' = 52$ $\mu F/m^2$ (from eq 4) while the measured value is $C_1'' = 75$ $\mu F/m^2$. Both measured values are in excellent agreement with the predictions.

We turn now to the observed phase shifts $\Delta\Phi$ over nanowire samples. Using the model of Figure 3b, the capacitance of the SWNT to each metal plate separately is found analytically[8] and then combined in series to give $C_2(h)$. We find $C_2''(h) > C_1''(h)$ for all scan heights $h = 10-100$ nm (Figure 4a). Thus eq 3 predicts a *negative* phase shift, in agreement with the measurements. The quantitative agreement is very good for intermediate scan heights ($h = 30-50$ nm) where the model geometry is appropriate.

Following ref 1, we plot the data as $|\Delta\Phi|^{-1/2}$ vs L^{-1} (blue points in Figure 4b). In contrast to ref 1, the data do *not* lie on a straight line but rather show a slight upward curvature. This dependence is reflected very well in the predictions of the model for our sample parameters (green line in Figure 4b). The authors of ref 1 found an almost perfect linear dependence in their experiment. Although compatible with their measurements, the simpler model they proposed did not predict the value of the slope or intercept. We find that with the experimental parameters of ref 1 ($h = 120$ nm, $t = 1$ μm), our quantitative model accurately reproduces the linear dependence, with a slope and intercept that are within a factor of 2 of this earlier experiment. Given that the scan height of 120 nm is outside the model's range of accuracy, we find this agreement to be satisfactory.

For PEO fiber samples, the geometry of Figure 3c yields

$$C_2''(h) = 2\epsilon_0(\pi R_{tip}^2)\frac{1}{(h + t/\epsilon_S + D/\epsilon_f)^3} \qquad (5)$$

where ϵ_f is the fiber dielectric constant. Equation 3, 4, and 5 predict that the phase shift for insulating nanofibers is always *positive* (as observed; see Figure 1c) since $C_2''(h) < C_1''(h)$.

As an important practical application, we use the model to determine the dielectric constant ϵ_f of PEO [$(CH_2-CH_2-O)_n$] nanofibers. From the slope of the plot of $\tan(\Delta\Phi)$ vs V_{tip}^2 (Figure 2d) and eqs 3−5 we find the fiber dielectric

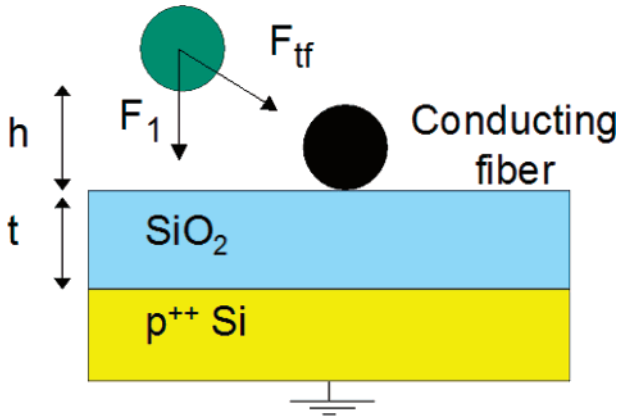

Figure 5. Schematic of the interaction between the AFM tip and the conducting fiber. The additional force F_{tf} leads to a negative phase shift when the tip is at a lateral position from the sample.

constant (at the cantilever oscillation frequency of 48 kHz) to be $\epsilon_f = 2.88 \pm 0.12$ (we use measured or manufacturer quoted values $Q = 150$, $k = 0.65$ N/m, $R_{tip} = 30$ nm, $\epsilon_S = 3.9$, $t = 190$ nm, PEO fiber diameter $D = 25$ nm). We have not found another measurement of this quantity in the literature. However, our measured value is between the tabulated dielectric constants for polyethylene $(CH_2-CH_2)_n$, $\epsilon_{PE} = 2.28$ to 2.32, and that for polyoxymethylene $(CH_2-O)_n$, $\epsilon_{POM} = 3.6$ to 4 at 1 kHz and room temperature.[9] This is consistent with the higher polarizability of the C−O bond compared to that of the C−C bond. As expected, the measured value is also higher than $\epsilon_{PEO} = 2.24$ found for PEO at optical frequencies.[10]

Finally, we explain the negative-positive-negative ("double dark line") phase shift observed for conducting PAn.HCSA/PEO nanofiber (Figure 1d). The fact that this contrast is seen only for conducting fibers, and not for insulating PEO fibers of equal diameter, rules out the possibility that it is an artifact of crosstalk from the topography signal. To explain the negative phase shift we note that as the tip approaches the conducting nanofiber from the side at height h above the substrate, two forces act on the cantilever: the capacitive force from the tip−substrate interaction F_1 and an additional *attractive* force F_{tf} due to the tip−fiber interaction (Figure 5). This additional force leads to a *decrease* in the phase Φ (from eq 2, $\tan(\Phi) = -(Q/k)(F_1' + F_{tf}') < \tan(\Phi_0) = -(Q/k)F_1'$) and thus to a negative phase shift $\Delta\Phi$. When the tip is directly above the fiber, the phase shift is due to the capacitive coupling between tip and nanofiber (eq 3). Since the diameter of the conducting fiber ($D = 80-150$ nm) is larger than the tip radius, we model the tip and sample as a sphere above a metallic plate and find that $C_2''(h) < C_1''(h)$, for all scan heights $h = 10-500$ nm, leading therefore to a positive phase shift above the conducting fiber. Although this model explains qualitatively the negative-positive-negative phase shift, the numerical predictions are typically a factor of 2−3 larger than the data. This suggests that the exact geometry of the conducting nanofiber should be taken into account in order to quantitatively explain the measurements.

In conclusion, we have developed a quantitative model for phase shifts in SCM based on the change in the total capacitance of the tip−sample−substrate system. We use simple geometric models and find excellent agreement with data collected on SWNTs and insulating PEO nanofibers. The "negative-positive-negative" phase shift for conducting nanofibers is explained by modeling the tip−fiber system as a sphere above a metallic plate. Finally, we have shown that the model can be combined with SCM data to measure the dielectric constant of nanoscale PEO fibers. This method is general and can be used to determine the dielectric constant of other insulating nanowires.

Acknowledgment. We acknowledge Mohammad Islam for helpful discussions. This work was supported by the Laboratory for Research on the Structure of Matter (NSF DMR00-79909) and the National Science Foundation NIRT (PHY-0103552).

References

(1) Bockrath, M.; Markovic, N.; Shepard, A.; Tinkham, M.; Gurevich, L.; Kouwenhoven, L. P.; Wu, M. W.; Sohn, L. L. *Nano Lett.* **2002**, *2*, 187.
(2) Zhou, Y.; Freitag, M.; Hone, J.; Staii, C.; Johnson, A. T.; Pinto, N. J.; MacDiarmid, A. G. *Appl. Phys. Lett.* **2003**, *83*, 3800.
(3) Radosavljević, M.; Freitag, M.; Thadani, K. V.; Johnson, A. T. *Nano Lett.* **2002**, *2*, 761.
(4) Wiesendanger, R. *Scanning Probe Microscopy and Spectroscopy: Methods and Applications*; Cambridge University Press: Cambridge, 1994.
(5) Bonnell, D. A.; Huey, B. L. In *Scanning Probe Microscopy and Spectroscopy, Theory, Techniques and Applications*, 2nd ed.; John Wiley and Sons: New York, 2001; pp 8−42.
(6) Kalinin, S. V.; Bonnell, D. A. In *Scanning Probe Microscopy and Spectroscopy, Theory, Techniques and Applications*, 2nd ed.; John Wiley and Sons: New York, 2001; pp 205−251.
(7) Terris, B. D.; Stern, J. E.; Rugar, D.; Mamin, H. J. *Phys. Rev. Lett.* **1989**, *63*, 2669.
(8) Durand, E. *Électrostatique et Magnétostatique*; Masson: Paris, 1953; p 91.
(9) *Polymer Handbook*, 4th ed.; John Wiley and Sons: New York, 1999.
(10) Takahagi, T.; Saiki, A.; Sakaue, H.; Shingubara S. *Jpn. J. Appl. Phys.* **2003**, *42*, 157.

NL049748W